Steady-state and non-steady-state current flow in thin-film Al-CeF_3-Al samples*

J. G. Simmons
Electrical Engineering Department, University of Toronto, Toronto, Canada

G. S. Nadkarni
Precision Electronic Components Ltd., Toronto, Canada

(Received 3 March 1975)

An experimental study of steady-state and non-steady-state current-voltage characteristics of thin-film Al-CeF_3-Al samples is presented. At high temperatures where steady-state conditions prevail, the I-V characteristics are observed to be independent of the insulator thickness, and to obey the relationship $\log_{10} I \propto V^{1/4}$. At low temperatures, where non-steady-state conditions prevail, the I-V characteristics are no longer uniquely determined, but rather depend on the voltage V_d applied during cooling. Furthermore, *negative* currents are observed to flow in the system when $V < V_d$, and *positive* currents for $V > V_d$; no current flows in the system when $V \approx V_d$. In all cases it is found that the conduction process is bulk limited, and the I-V characteristic is characterized by $\log_{10} I \propto V^{1/2}$. The results are interpreted in terms of Schottky barriers existing at the metal-insulator interfaces. Excellent correlation is obtained between the steady-state and the non-steady-state theory and experiment. The trap parameters used in generating the theoretical characteristics are consistent with those obtained from previous thermal and isothermal dielectric relaxation current studies. In view of these studies it is concluded that steady-state uniform-field concepts cannot be generally applied to the analysis of the experimental data on metal-insulator-metal systems, and that any previous analysis of data that has involved such concepts should be viewed with caution.

I. INTRODUCTION

It is often observed in thin-film metal-insulator-metal (MIM) systems that the current is an exponential function of the applied voltage, and it appears to have been almost an article of faith to assume that the system is in the steady state and to use uniform-field concepts when analyzing the data. By uniform-field concepts we mean that the field is assumed to be uniform throughout the insulator before and after the voltage is applied to the system, as shown in Fig. 1. Hence, the field throughout the insulator is usually assumed to be zero under zero-bias condition, and to be equal to V/L when a voltage V is applied to the system, where L is the insulator thickness. Basically, what this means is that any possible interactions between the metal electrodes and the defect insulator are ignored, yet insulators containing high trap densities or high ion concentrations can give rise to pronounced Schottky barriers at the metal-insulator interface.[1-3] The data of Stuart[5] and Hartman *et al.*,[4] obtained from SiO films with Al and Au electrodes, have been interpreted in terms of Schottky-barrier effects. The existence of Schottky barriers at the interfaces of MIM systems has been confirmed experimentally by ac,[6-8] stimulated dielectric relaxation currents[9,10] (SDRC), and isothermal dielectric relaxation current measurements[11] (IDRC).

We show that uniform-field concepts are not applicable to MIM systems containing Schottky barriers. Consequently, neither the conventional Schottky characteristics for electrode-limited current flow

$$I \propto \exp[(\beta/kT)(V/L)^{1/2}], \tag{1}$$

or the Poole-Frenkel characteristics for bulk-limited current flow

$$I \propto \exp[(2\beta/kT)(V/L)^{1/2}], \tag{2}$$

apply to such systems. In Eqs. (1) and (2), k is Boltzmann's constant,

$$\beta = (q^3/4\pi\epsilon)^{1/2}, \tag{3}$$

where q is the unit electronic charge, and ϵ is the permittivity of the insulator. Furthermore, recent SDRC and IDRC theoretical[12-13] and experimental studies[9-11] have clearly shown that non-steady-state processes often dominate steady-state processes, particularly at low temperatures. We will show here that these phenomena have a striking effect on the I-V characteristics.

II. PHYSICAL PRINCIPLES

When a voltage V_d is applied to an MIM system containing Schottky barriers, immediately thereafter the applied voltage is uniformly distributed throughout the insulator {Fig. 2[a(ii)]}, and the system is in the nonsteady state. In this case, the field F_i in the interior is given by $F_i \simeq V_d/L$. Ultimately, the system will decay to the steady state illustrated by the energy diagram in Fig. 2[a(iii)]. In the steady state, most of the applied voltage is dropped across the reverse-biased (cathodic) Schottky barrier, and the remainder across the

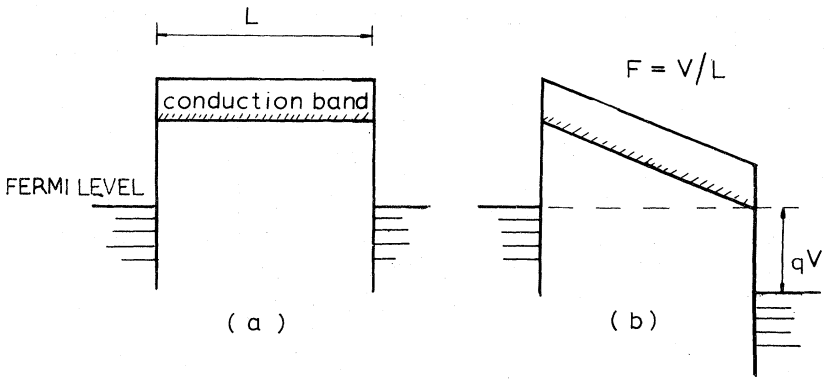

FIG. 1. Energy diagram for an idealized MIM system illustrating the uniform-field concept: (a) represents zero-bias condition and (b) represents voltage bias condition. Note that the field in the insulator is V/L.

interior (neutral region) of the insulator and the forward-biased (anodic) Schottky barrier. Furthermore, the cathodic depletion region increases in size (from λ_0 to λ_c) as a result of the system relaxing to the steady state.

The time t_r required for the system to relax from the nonsteady state to the steady state depends upon the emission probability e_n of electrons from the trap levels to the conduction band of the insulator, which probability is a strong function of temperature. For a discrete trap level

$$t_r \simeq e_n^{-1} = \nu^{-1} \exp[(E_c - E_t + \Delta E_t)/kT], \tag{4}$$

where ν is the attempt-to-escape frequency, E_t is the *zero-field* trap depth, and ΔE_t is the Poole-Frenkel reduction of the trap depth

$$\Delta E_t = 2\beta F_i^{1/2}, \tag{5}$$

where F_i is the field in the interior of the insulator.

If the sample is first cooled to a low temperature, or the trap depth is deep enough that $e_n \ll 1$, i.e., $t_r \gg 1$, and then the voltage is applied, the device will be in the non-steady-state condition depicted by Figs. 2[a–c(ii)]. In this case, the non-steady-state current is *bulk limited* and given by[12]

$$I_{\mathrm{IDRC}} \simeq I_0 \exp[-(E_t - 2\beta F_i^{1/2})/kT], \tag{6}$$

where

$$I_0 = qN_c A \mu F_i, \tag{7}$$

q is the unit of electronic charge, N_c is the effective density of state in the conduction band, A is the sample area, and μ is the electron mobility. Thus, since in this case, $F_i = V/L$, Eq. (6) has the same form as Eq. (2) and thus may be misinterpreted as being due to *steady-state* conduction in an MIM system with *neutral* contacts (Fig. 1).

At sufficiently high temperatures, such that $e_n \gg 1$, and $t_r \ll 1$, the system relaxes quickly to the steady state, and the current is dominated by electron flow across the cathodic interface. When this situation prevails the conduction process is electrode limited (i.e., thickness independent). In general, the steady-state–electrode-limited (Richardson-Schottky) current can be expressed in the form

$$J_{\mathrm{RS}} = A^* T^2 \exp[-(\phi_0 - \Delta\phi)/kT], \tag{8}$$

where A^* is Richardson's constant (120 A/cm^2), ϕ_0 is the ideal cathodic interfacial barrier height (see Fig. 2), and $\Delta\phi$ is the Schottky (image-effect) lowering of the barrier. In the case of an MIM sys-

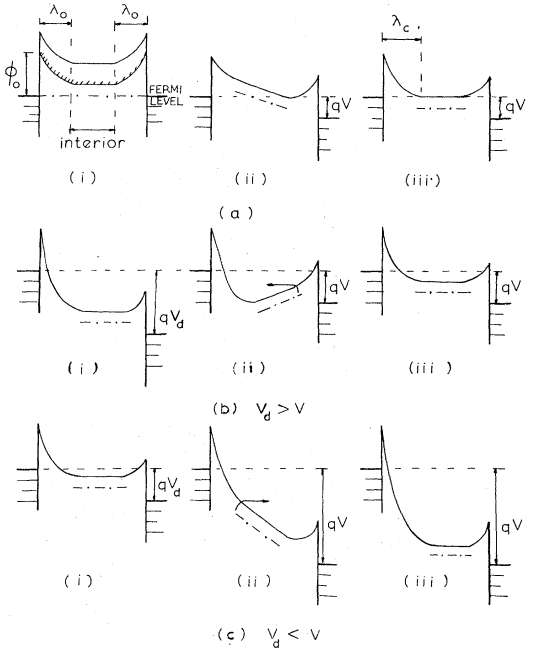

FIG. 2. Energy diagram for an MIM system containing interfacial Schottky barriers under various voltage bias: [a(i)], [b(i)], and [c(i)] are steady-state diagrams for initial voltage bias of zero, V_d and V_d, respectively. [a(ii)], [b(ii)], and [c(ii)] are *non-steady-state* diagrams immediately after voltage bias is changed from initial conditions (i) to a value V volts. [a(iii)], [b(iii)], and [c(iii)] represent *steady-state* conditions corresponding to the V volts. Note that the field E_i in the interior of the insulator under non-steady-state conditions (ii) is $|V - V_d|/L$, as will be apparent from simple geometric considerations.

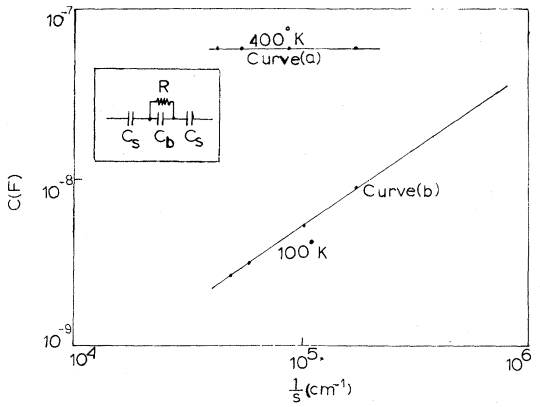

FIG. 3. Capacitance vs inverse thickness at two different temperatures. Inset illustrates the equivalent circuit for the sample.

tem containing Schottky barriers and a discrete trap level, $\Delta\phi$ is given by[1]

$$\Delta\phi = \beta F_c^{1/2}, \tag{9}$$

$$F_c = [(2qN_t/\epsilon)(\Delta\psi + V)]^{1/2}. \tag{10}$$

Hence

$$\Delta\phi = [(V + \Delta\psi)q^7 N_t/8\pi^2\epsilon^2]^{1/4}, \tag{11}$$

where N_t is the trap density and $\Delta\psi$ is the difference in the energies (eV) of the work functions of the electrode and insulator.

III. EXPERIMENTAL TECHNIQUE

A. Sample fabrication

The samples were fabricated on a glass substrate by the vacuum deposition of successive layers of aluminum, cerous fluoride (CeF_3), and aluminum. The deposition was made at a pressure of less than 10^{-5} Torr. The first electrode was deposited in the form of a strip 4.5 cm long and $\frac{1}{8}$ in. wide. The cerous fluoride was then deposited at a rate of about 8 Åsec^{-1}. Finally, the counter electrodes were deposited perpendicular to the lower electrode in the form of strips $\frac{1}{8}$ in. wide and 1.5 cm long so as to produce ten Al-CeF_3-Al capacitors on the substrate. The devices were completed without breaking the vacuum at any time. The thickness of the electrodes was about 1000 Å, and the thickness of the CeF_3 ranged locally in steps from 600 to 2000 Å on the substrate. The active area of the samples was 0.1 cm^2.

B. Electrical measurements

The current was measured using a Keithley (610C) electrometer and the temperature of the sample was measured with a copper-Constantan thermocouple located next to the sample under study. The measurements were carried out with the sample enclosed in Dewar evacuated to 10^{-3} Torr, in order to minimize the deleterious effect of the ambient gases.

IV. ac MEASUREMENTS

Figure 3 illustrates the capacitance as a function of inverse thickness. Curve *a* was obtained at 400 °K and it is seen that the capacitance is essentially independent of thickness. Curve *b* was obtained at 100 °K, and in this case the capacitance is seen to be inversely proportional to thickness.

These results offer striking evidence for the existence of Schottky barriers at the metal-insulator interfaces.[6-8,14] Briefly, the results can be explained in terms of the proposed equivalent circuit shown in the inset of Fig. 3. The two capacitors C_S represent the capacitance of the Schottky barriers being assumed to be perfectly blocking. C_b and R_b represent the capacitance and resistance of the neutral bulk (interior) of the insulator, respectively; R_b may be expressed in the form $R_b = R_0 e^{\phi_b/kT}$, where ϕ_b is the activation energy of the insulator interior. At low temperature R_b is very large. Hence, the capacitance of the system is simply the series capacitance of the two Schottky-barrier capacitances and the bulk capacitance or simply the geometric capacitance which, of course, is inversely proportional to sample thickness, as observed. At high temperatures R_b is low and essentially shunts C_b. Thus, the capacitance is now simply the series capacitance of the two Schottky barriers. Since the widths of the Schottky barriers are constant in samples prepared under identical conditions, then the capacitance is independent of the sample thickness.

From the low-temperature characteristic we obtain the dielectric constant to be 9.5, and using this value in conjunction with the high-temperature data we obtain the thickness of the Schottky barriers to be approximately 60 Å.

V. ISOTHERMAL *I-V* CHARACTERISTICS

A. Steady-state results

In order to obtain the steady-state *I-V* characteristics, the voltage was applied to the sample at high temperature ($T = 320$ °K and $e_n \gg 1$), so that it quickly relaxed to the steady state {Fig. 2[a (iii)]}.

Figure 4 illustrates the steady-state *I-V* curve plotted as $\log_{10} I$ vs V and $\log_{10} I$ vs $(0.8 + V)^{1/4}$. These characteristics were found to be essentially independent of the insulator thickness. These data conform to the relationship[15]

$$\log_{10} I \propto (0.8 + V)^{1/4}. \tag{12}$$

A similar relationship has been observed recently by Caserta and Serva.[16] Relation equation (12) is consistent with Eq. (8); that is the current can be expressed in the form

$$J_{RS} = D\exp(1/kT)\{[(0.8+V)C]^{1/4} - 1.5\}\ \text{A/cm}^2, \quad (13)$$

where $D \simeq 7\times10^6$ A/cm^2 and $C \simeq 2.1\times10^{-1}$ eV^3.

From an inspection of Eqs. (8), (11), and (13), we deduce directly that $\Delta\psi \simeq 0.8$ eV and $\phi_0 = 1.5$ eV. From the value of C in Eq. (13) we compute $N_t \simeq 5\times10^{19}$ cm^{-3}, which is in reasonable agreement with previous DRC data.[9,11] Since $T = 320$ °K, we have $A^* = D/T^2 \simeq 88$ A/cm^2 K^2 and in excellent agreement with practical values.[17,18] Also, the actual barrier height $\phi_0 - \Delta\phi$ for $V = 1.5$ V is computed to be 1.0 eV, which is in excellent agreement with previous SDRC measurements. In view of the above results, we conclude that Schottky barriers exist in the electrode-insulator interface.

B. Non-steady-state results

Non-steady-state measurements were made by first applying a voltage V_d at high temperature, so that the sample relaxed quickly to the steady state. The sample was then cooled to a predetermined constant low temperature T_0 with V_d still applied, and at that temperature the I-V characteristics were generated. The results of this procedure are shown in Figs. 5 and 6, which illustrate the non-steady-state I-V characteristics for several values of V_d at $T_0 = 240$ °K (Fig. 5) and $T_0 = 225$ °K (Fig. 6).

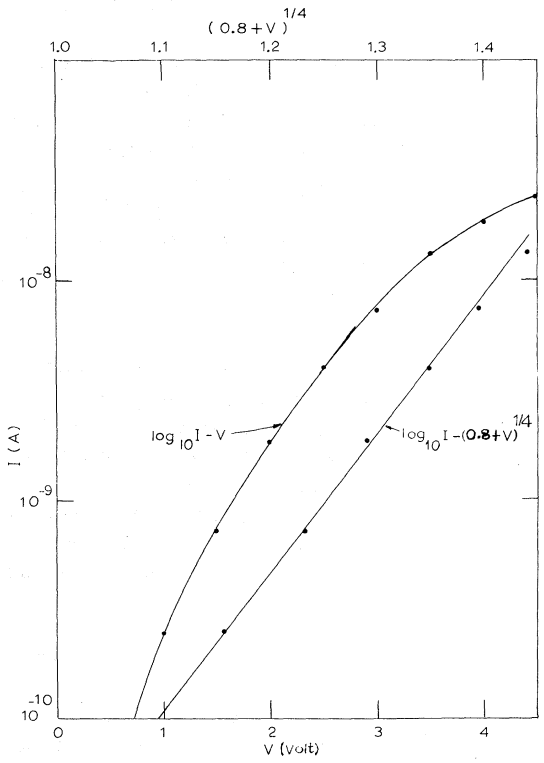

FIG. 4. Steady-state $\log_{10} I$-vs-V and $\log_{10} I$-vs-$(0.8+V)^{1/4}$ characteristics for $T = 320$ °K. Insulator thickness is 1800 Å.

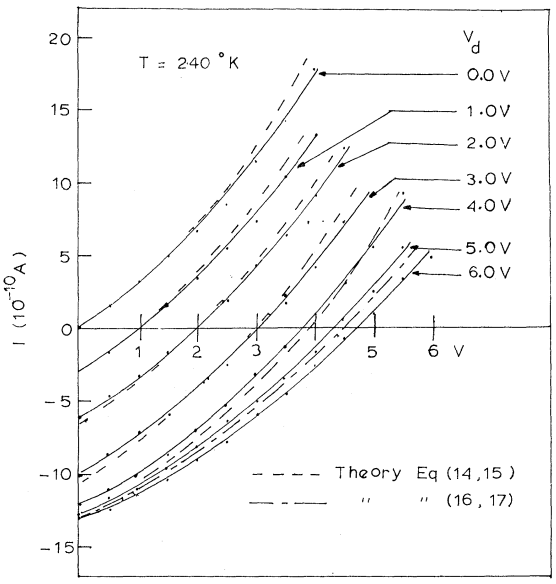

FIG. 5. Family of non-steady-state I-V characteristics for $T = 240$ °K with V_d as a parameter. Theoretical curves for Eqs. (16) and (17) are for $V_T = 4.5$ V.

The interesting features of the characteristics shown in Figs. 5 and 6 are (a) the I-V characteristics are not uniquely defined, but depend upon V_d the initial voltage; (b) for $V < V_d$ a *negative* current flows in the sample, i.e., the direction of the cur-

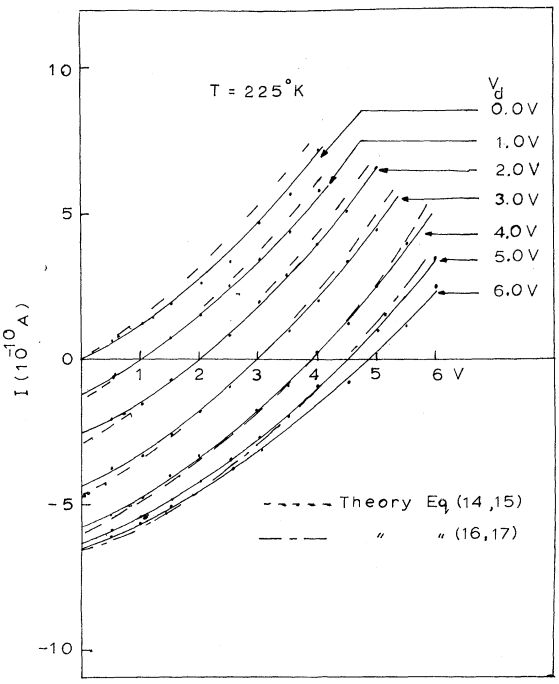

FIG. 6. Family of non-steady-state I-V characteristics for $T = 225$ °K with V_d as a parameter. Theoretical curves for Eqs. (16) and (17) are for $V_T = 4.5$ V.

rent flow is in the *opposite* direction to the conventional current flow; (c) the current is *zero* for $V \simeq V_d$ when $V_d \lesssim 4$ V, and the I-V curves for various V_d are essentially parallel; and (d) for $V_d > 5$ V the I-V characteristics are essentially identical, i.e., independent of V_d.

These results can be readily explained on the basis that Schottky barriers and non-steady-state conditions exist in the sample as follows: on the application of the voltage at high temperature, the system relaxes to the steady state as shown by group (i) energy diagrams in Figs. 2(a)–2(c). Now, provided the voltage is held constant during cooling, the system will be in the steady state at low temperatures. If, however, the voltage is deviated from V_d [see group (ii) of Figs. 2(a)–(c)] after the sample is cooled, a non-steady-state current flow will be induced in the system. Provided that the temperature is sufficiently low so that $e_n \ll 1$ ($t_r \gg 1$), then the non-steady-state current will be essentially constant in time.[12] *Thus, an I-V characteristic measured at low temperatures, although apparently steady state is, in fact, nonsteady state in nature.*

For $V < V_d$ the energy diagram for the non-steady-state condition will be as shown in Fig. 2[b(ii)]. In this case, it will be noted that the field in the interior of the insulator, which is equal to $(V - V_d)/L$, is such as to drive electrons in the interior from the anode towards the cathode. In other words, reducing the voltage below V_d causes negative currents to flow, as is observed. For $V > V_d$, the field in the interior is now such as to drive the electrons in the interior from the cathode to the anode; that is, a conventional non-steady-state current flows in the system in this case. Because the non-steady-state currents are considerably greater than the steady-state currents,[9] it requires that the voltage only be decreased *slightly* below V_d, to induce a negative non-steady-state current capable of neutralizing the conventional current flowing over the cathodic barrier. What this means is that for V just slightly less than V_d ($V \simeq V_d$), the current in the system is zero, as is observed. The above statements are summarized by the following equations [cf. Eq. (6)]:

$$I_{\mathrm{SDRC}} = -I_0 \exp[-(E_t - 2\beta F_i^{1/2})/kT], \quad V_d > V \tag{14}$$

and

$$I_{\mathrm{SDRC}} = I_0 \exp[-(E_t - 2\beta F_i^{1/2})/kT], \quad V_d < V, \tag{15}$$

where $F_i = |V_d - V|/L$.

Equations (14) and (15) are shown plotted as dashed curves in Figs. 5 and 6 using $E_t = 0.68$ eV as computed from previous SDRC measurements.[9] For $V \leq 4.5$ V, the correlation is very good and clearly shows the non-steady-state–bulk-limited nature of the I-V characteristics, which is to be contrasted with the electrode-limited nature of the steady-state characteristics.

The reason that the characteristics become independent of $V_d \geq 4$ V is explained as follows: the discussion given above assumes that the cathodic contact is blocking at all values of V_d. However, it has been shown in previous studies[9] on similar samples that above a certain threshold voltage V_T, the conduction process undergoes an electrode-limited to bulk-limited transition.[1] What this means as far as we are concerned here, is that for voltages above V_T, only a small fraction of the applied voltage in excess of V_T appears across the cathodic barrier, the majority being absorbed by the interior of the insulator. Clearly then, since the maximum voltage that can be maintained across the cathodic barrier is approximately V_T, it follows from the previous reasoning that for $V_d \gtrsim V_T$ the current will cease to flow in the device when $V \simeq V_T$. The above statement is summarized in the following equations:

$$I_{\mathrm{SDRC}} = -I_0 \exp\{-[E_t - 2\beta(F_i')^{1/2}]/kT\}, \quad V < V_T, \quad V_d > V_T, \tag{16}$$

$$I_{\mathrm{SDRC}} = I_0 \exp\{-[E_t - 2\beta(F_i')^{1/2}]/kT\}, \quad V > V_T, \quad V_d > V_T, \tag{17}$$

where $F_i' \simeq |V_T - V|/L$. Equations (16) and (17), which are independent of V_d, are shown plotted in Figs. 5 and 6.

From the above arguments, it will be evident that manifestation of the onset of the electrode-limited–to–bulk-limited transition is when the condition for zero current in the sample begins to deviate from $V \simeq V_d$. Hence, from Figs. 5 and 6, the onset of this transition occurs approximately at about 4.5 V, which value is in good agreement with that obtained from SDRC studies.[9]

VI. CONCLUSIONS

This study illustrates the profound effects of Schottky barriers on the electrical properties of Al-CeF_3-Al samples. It has been shown that at high temperatures a steady-state *electrode-limited* conduction process prevails from which the *ideal* cathodic interfacial barrier height has been determined to be approximately 1.5 eV, and the trap density to be 5×10^{19} cm^{-3}, which values are in good agreement with previous SDRC,[9] IDRC,[10] and ac[19] studies.

At low temperatures, a non-steady-state bulk-limited conduction process prevails and, consequently, the I-V characteristic is not uniquely determined but is a function of voltage applied to the sample during cooling. Furthermore, for voltages $V_d \geq 4.5$ V there is an electrode-limited transition in the conduction process.

The correlation between steady-state and non-steady-state theory and experiment is excellent. Consequently, it is concluded that steady-state–uniform-field concepts are not applicable to the case in hand. We would also add that in view of the evidence presented here any previous analysis of the experimental data obtained from MIM systems that have been carried out assuming steady-state uniform-field concepts should be viewed with caution.

---

*Study supported in part by National Research Council and Defence Research Board of Canada.

[1]J. G. Simmons, Phys. Rev. 166, 912 (1968).
[2]J. G. Simmons, J. Phys. Chem. Solids 32, 2581 (1971).
[3]-J. Maserjian and C. A. Mead, J. Phys. Chem. Solids 28, 1957 (1968); 28, 1971 (1968).
[4]T. C. Hartman, J. C. Blair, and R. Bauer, J. Appl. Phys. 37, 2464 (1966).
[5]M. Stuart, Phys. Status Solidi 23, 595 (1967).
[6]J. G. Simmons and G. S. Nadkarni, J. Vac. Sci. Technol. 6, 12 (1969).
[7]G. S. Nadkarni and J. G. Simmons, J. Appl. Phys. 41, 545 (1960).
[8]G. S. Nadkarni and J. G. Simmons, J. Appl. Phys. 43, 3741 (1972).
[9]J. G. Simmons and G. S. Nadkarni, Phys. Rev. B 6, 4815 (1972).
[10]G. S. Nadkarni and J. G. Simmons, J. Appl. Phys. 43, 3650 (1972).
[11]G. S. Nadkarni and J. G. Simmons, Phys. Rev. B 7, 3719 (1973).
[12]J. G. Simmons and G. W. Taylor, Phys. Rev. B 6, 4793 (1972).
[13]J. G. Simmons and G. W. Taylor, Phys. Rev. B 6, 4804 (1972).
[14]J. G. Simmons, G. S. Nadkarni, and M. Lancaster, J. Appl. Phys. 41, 538 (1970).
[15]Data also conforms to a $\log_{10} J$-vs-$V^{1/2}$ relationship, but Eq. (12) is preferred because it fits in with the general analyses. Nor should it be construed that a $\log_{10} J$-vs-$V^{1/2}$ relationship suggests that Eqs. (1) or (2) may be applicable; this is because the data are *independent* of the insulator thickness.
[16]G. Caserta and A. Serva, Thin Solid Films 20, 91 (1974).
[17]A. Van der Ziel, *Solid State Physical Electronics* (Prentice-Hall, New York 1968), p. 141.
[18]C. Kittel, *Solid State Electronics*, (Wiley, New York, 1968), p. 247.
[19]A. Kalra, J. G. Simmons, and G. S. Nadkarni, J. Appl. Phys. (to be published).